Impact of wavy texture and hybridity of nanofluid on heat transfer augmentation over the frustum of cone geometry

Muhammad Saleem Iqbal[1], Abuzar Ghaffari[2], Irfan Mustafa[3], Hafiz Muhammad Ali[4*]

[1]*Department of Mathematics Islamabad College for Boys G-6/3, Islamabad 44000, Pakistan.*

[2]*Department of Mathematics, University of Education, Lahore (Attock Campus 43600), Pakistan.*

[3]*Department of Mathematics, Allama Iqbal Open University, H-8, Islamabad 44000, Pakistan.*

[4]*Mechanical Engineering Department, King Fahd University of Petroleum and Minerals, Dhahran 31261, Saudi Arabia*

* hafiz.ali@kfupm.edu.sa

Abstract

In this article, the impact of water-based hybrid nanofluid on heat transfer characteristics along the wavy frustum of the cone is examined. We considered hybrid nanofluid containing Cu and TiO_2 nanoparticles. Non-similar form of the constitutive equations is obtained by using an appropriate set of transformations and results are achieved by employing transformed into compact non-similar form and are solved by the famous numerically implicit finite difference scheme known as Keller-box technique. The influence of the hybrid nanoparticles' volume fraction, frustum of cone half-angle γ, and the wavy texture parameters on the Nusselt number and skin friction are scrutinized and comparison is made between the wavy frustum of the cone and flat frustum of the cone through numerical data. It is observed that the rise in the truncated cone half-angle leads to an increase in skin friction and Nusselt number. Titania – water nanofluid has lower heat transfer rates as compared to copper-titania hybrid nanofluid. The increasing of the truncated cone half-angle enhances the heat transfer rates. Generally, the results established from this analysis can be used as a benchmark for improving the natural convection heat transfer performance along the frustum of cone wavy texture.

Keywords: Wavy surface; Frustum of cone; Keller box scheme; Non-similar equations

1. Introduction

The science and phenomena of heat transfer enhancement, or intensification, or increase, have been established into the significant aspect of various topographies of engineering and thermal science. The collected literature in the enhancement of heat transfer contains thousands of references, and it continues to grow continuously. It is a substantial challenge for the dissemination of applicable design and relevant information.

Natural convection heat transfer phenomena are encountered in many fields of industry and engineering. Due to economic advantage, low noise, and simple technique several investigators debated the natural convective phenomena about the vertical frustum of a cone in Newtonian fluids. The process of heat transfer due to natural convection phenomena over a frustum of a cone is appropriate in many types of thermal design apparatus, for example, nuclear reactor, dehydration process in chemical and food process, steam generators, cooling solar energy plants, heat exchangers, drying and geothermal reservoirs. Pioneer work on flat frustum of a cone geometry for natural convection for CWT and CHF cases were conducted by Na and Chiou [1-2]. Singh et al. [3-4] discussed the constant wall heat flux case, using the local non-similarity method. Pop and Na [5] studied natural convection over a vertical frustum of the cone in a porous medium. Yih [6] studied the effect of radiation on free convection about a truncated cone. Chamkha [7] investigated MHD free convection flow about a truncated cone in the presence of radiation effects. Hossain et al [8] studied the impact of variable thermophysical properties on the natural convection flow of a truncated cone. Postelnicu [9] explored the free convection about a vertical frustum of a cone in a micropolar fluid. Cheng [10-12] studied the influence of variable properties and power-law variation in surface temperature on natural phenomena along vertical truncated cone for micropolar fluid in the porous regime. Srinivasa and Eswara [13] explored the influence of heat generation/absorption and MHD on convective flow over the truncated cone and seen that increasing heat generation/absorption parameter corresponds to a decrease in the heat transfer coefficient.

Convective heat transfer is an essential phenomenon in several engineering processes such as electronic cooling, heat exchangers, and thermal power plants. Base fluids like water, ethylene glycol mixture, and oil have low thermal conductivity, consequently the weak heat transfer fluids. By the addition of nanophase particles in these fluids, the heat transfer phenomena of the base fluid can be boosted. This is because the addition of nanoparticles upturns the heat capacity and surface area of the fluid, the random motion of nanoparticles increases the temperature gradient of the fluid.

In the current two decades, several authors discussed convective heat transfer phenomena with nanofluids. Cheng [14] investigated free flow in a bi-disperse porous regime and shown that increasing the modified thermal conductivity ratio increases the heat transfer phenomena. Patrulescu et al. [15] studied mixed convection nanofluid flow over a vertical frustum of a cone and shown that an increase in the mixed convection parameter decreases the heat transfer characteristics. Siddiqa et al. [16] discussed two-phase dusty fluid flow over a vertical frustum of a cone and concluded that the rate of heat transfer rate significantly increases by the inclusion of nanoparticles. Amanulla et al. [17] examined Casson nanofluid past a truncated cone texture and analyzed that the buoyancy ratio parameter increases the fluid flow. Ahmed and Mahdy [18] analyzed variable physical propertied for MHD natural convection nanofluid flow past a truncated cone and found that by increasing MHD leads to an increase in the rate of heat transfer. Siddiqa et al. [19] reported the radiative heat transfer for two-phase Casson dusty fluid flow over truncated vertical cone and shown that the radiation strongly affects the heat transport phenomenon.

The wavy texture corresponds to the increased surface area which supports the convective heat transfer phenomena. The investigation of the heat transfer process with non-flat texture is particularly significant in many usages. The heat transfer phenomenon is strongly influenced by the form of the apparatus. The periodic functions like sine and cosine functions support the mathematical formation. Moreover, fluids having high conductivity such as nanofluid are the best suitable way to enhance the convective phenomena. Siddiqa et al. [20] reported gray dusty fluid flow along a vertical wavy frustum of a heated cone and analyzed that the rate of heat transfer coefficient considerably upturns for contaminated air. Siddiqa et al. [21] analyzed non-linear radiative flow along the wavy cone surface and shown that It is found that the rate of heat transfer reduces with increasing surface radiation parameters.

Mahdy and Elshehabe [22] studied nanofluid convective flow due to gyrotactic microorganisms past vertical truncated cone in a porous regime and concluded that rescaled velocity depends significantly on the bio-convection parameter. Reddy and Rao [23] explored that nanofluid flow over the frustum of a cone in the doubly stratified non-Darcy porous regime and found that reduction in velocity of fluid flow is observed as the non-Darcy parameter increases.

In this article, the heat transfer analysis is investigated for free convection past a wavy vertical frustum of a cone in hybrid nanofluid using Tiwari and Das model. The flow is incompressible, steady, and laminar. By taking frustum of cone half-angle so large that curvature effects are neglected. Using the above-mentioned assumptions, constitutive PDEs are formulated and converted to non-similar parabolic PDEs by an appropriate set of transformations. A direct numerical solution is obtained by the Keller-box method. Tables and graphs are displayed are for flow characteristics and heat transfer rates. Before analysis, for conformation of code calculated results are matched with the available data and seen that these values are in superb matching.

Important physics, primary understanding, and beneficial contributions to the analysis of convection phenomena in fluid flow along wavy texture are given in ref. [24-30].

The objective of this research article to consider the impact of hybrid nanofluid on the flow and heat transfer characteristics in a natural convection flow over an isothermal wavy truncated cone.

2. Problem statement and mathematical formulation

Two dimensional Newtonian free convective flow past vertical truncated cone of wavy texture. The nature of wavy texture is sinusoidal and its mathematical form is taken as$\bar{y}_w = \bar{S}(\bar{x}) = \bar{\alpha} sin\left(\frac{\pi\bar{x}-\bar{x}_0}{l}\right)$; slant height at the lower end of the truncated cone is $\bar{x}_0$, the wave length is l, and fixed amplitude is $\bar{\alpha}$. The geometry of the truncated cone of wavy texture is displayed in Figure 1. $O(\bar{x} = \bar{y} = 0)$ is the leading edge (apex), $\bar{x}$ and $\bar{y}$ is along and perpendicular to truncated cone surface Flat surface and local radius $\bar{r}$ of the truncated cone and related through $\bar{r}(\bar{x}) = (\bar{x} + \bar{x}_0)sin\beta$; β is the truncated cone half-angle. The valid boundary constraints for this problem are

$$\begin{aligned} &\bar{y} = \bar{S}(\bar{x}): T = T_w, \quad \bar{u} = 0, \quad \bar{v} = 0, \\ &\bar{y} \to \infty: \bar{u} = 0, \quad T = T_\infty, \quad \bar{p} = p_\infty, \\ &\bar{x} = 0: T = T_\infty, \ \bar{p} = p_\infty, \text{ for all } \bar{y} \neq 0. \end{aligned} \tag{1}$$

where p_∞, T_∞ are the ambient pressure and temperature of fluid, and T_w $(T_w > T_\infty)$ is the surface temperature.

Here we are using Tiwari and Das model [31] because it is the most appropriate that during convective transport in nanofluid it explains the nanoparticle contribution in heat transfer phenomena. This model incorporates the thermophysical properties of the nanofluid and the relations for these properties are listed in Table1. The nanoparticles used in this analysis are Cu and TiO_2 and their numerical values are recorded in Table 2. The governing consecutive equations according to Tiwari and Das model, the two-dimensional mass, momentum, and energy conservation laws are given by

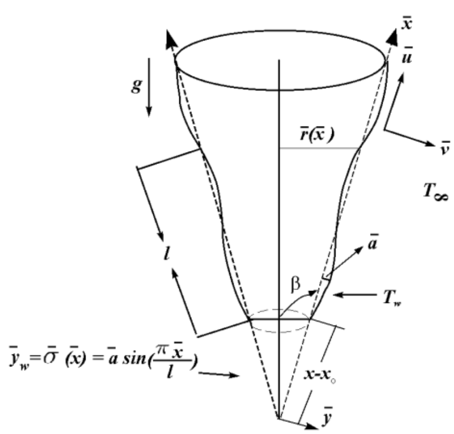

Figure 1: Physical model and coordinate system.

$$\frac{\partial(\bar{r}\bar{u})}{\partial\bar{x}}+\frac{\partial(\bar{r}\bar{v})}{\partial\bar{y}}=0, \tag{2}$$

$$\bar{u}\frac{\partial\bar{u}}{\partial\bar{x}}+\bar{v}\frac{\partial\bar{u}}{\partial\bar{y}}=-\frac{1}{\rho_{nf}}\frac{\partial\bar{p}}{\partial\bar{x}}+\nu_{nf}\nabla^2\bar{u}+\frac{1}{\rho_{nf}}g(\rho\beta^*)_{nf}(T-T_\infty)sin\beta, \tag{3}$$

$$\bar{u}\frac{\partial\bar{v}}{\partial\bar{x}}+\bar{v}\frac{\partial\bar{v}}{\partial\bar{y}}=-\frac{1}{\rho_{nf}}\frac{\partial\bar{p}}{\partial\bar{y}}+\nu_{nf}\nabla^2\bar{v}+\frac{1}{\rho_{nf}}g(\rho\beta^*)_{nf}(T-T_\infty)cos\beta, \tag{4}$$

$$\bar{u}\frac{\partial T}{\partial\bar{x}}+\bar{v}\frac{\partial T}{\partial\bar{y}}=\alpha^*_{nf}\nabla^2 T, \tag{5}$$

where ${\beta^*}_{nf}$, ρ_{nf}, α^*_{nf}, $(\rho c_p)_{nf}$, $\rho\kappa_{nf}$ are, respectively, the thermal expansion coefficient, density and thermal diffusivity of the nanofluid, heat capacitance, thermal diffusivity, and thermal conductivity of the nanofluid which are directly related to the nanoparticle volume fraction. The relations transformed for regular fluid by selecting nanoparticle volume fraction equal to zero. Moreover, ∇^2 is the Laplacian operator, $(\bar{u},\bar{v})$ is velocity vector along $(\bar{x},\bar{y})$ directions and g be the gravitational acceleration. Introducing a group of proper dimensionless variables presented by

$$\begin{gathered}\xi=x=\frac{\bar{x}}{l},y=\frac{\bar{y}-\bar{S}(\bar{x})}{l}Gr^{\frac{1}{4}},u=\frac{\rho_{fl}}{\mu_f}Gr^{-\frac{1}{2}}\bar{u}\ ,v=\frac{\rho_{fl}}{\mu_f}Gr^{-\frac{1}{4}}\left(\bar{v}-S_\xi\bar{u}\right),u=\frac{\partial\psi}{\partial x},\\ v=-\frac{\partial\psi}{\partial y}\ \ S=\frac{\bar{S}(\bar{x})}{l},\theta(\xi,\eta)=\frac{T-T_\infty}{T_w-T_\infty},\psi(\xi,\eta)=\xi^{\frac{3}{4}}f(\xi,\eta),\eta=\xi^{-\frac{1}{4}}y,\\ Pr=\frac{\nu_f}{\alpha_f},Gr=\frac{g\beta_f(T_w-T_\infty)l^3}{\nu_f^2},p=\frac{l^2}{\nu^2\rho_f}Gr^{-1/4}\,\bar{p},\qquad r(\xi)=(\xi+\xi_0)sin\beta.\end{gathered} \tag{6}$$

By considering surface waves so small as compared to boundary layer thickness and utilizing the transformations given in Eq. (6), The Eqs., (3-5) written in compact form as

$$\frac{\mathcal{H}^2}{\mathbb{Q}_1}\frac{d^3f}{d\eta^3}+\left(\frac{3}{4}+\frac{\xi}{\xi+\xi_0}\right)f\frac{d^2f}{d\eta^2}-\left(\frac{1}{2}+\frac{\mathcal{H}_\xi}{\mathcal{H}}\xi\right)\left(\frac{df}{d\eta}\right)^2+\frac{\mathbb{Q}_4(1-S_\xi tan\beta)}{\mathbb{Q}_2\mathcal{H}^2}\theta=\xi\left[\frac{df}{d\eta}\frac{\partial f'}{\partial\xi}-\frac{d^2f}{d\eta^2}\frac{\partial f}{\partial\xi}\right], \tag{7}$$

$$\frac{\mathbb{Q}\mathcal{H}^2}{\mathbb{Q}_3Pr}\frac{d^2\theta}{d\eta^2}+\left(\frac{3}{4}+\frac{\xi}{\xi+\xi_0}\right)f\frac{d\theta}{d\eta}=\xi\left[\frac{df}{d\eta}\frac{\partial\theta}{\partial\xi}-\frac{d\theta}{d\eta}\frac{\partial f}{\partial\xi}\right], \tag{8}$$

And boundary constraints in final solid form shown as

$$\theta(\xi,0)=1, \qquad f(\xi,0)=0, \qquad \frac{df}{d\eta}(\xi,0)=0,$$
$$\theta(\xi,\infty)=0, \qquad \frac{df}{d\eta}(\xi,\infty)=0. \tag{9}$$

where $\mathbb{Q}, \mathbb{Q}_1, \mathbb{Q}_2, \mathbb{Q}_3$ and $\mathbb{Q}_4$ are physical constant parameters recorded in Table 3, $\mathcal{H}=\sqrt{1+S_\xi^2}$ and $\mathcal{H}_\xi$ designate the wavy input and its derivative and Pr is the Prandtl number. The superscript '$'$' and subscript 'ξ state differentiation w.r.t η and'ξ'respectively. The local skin friction coefficient and the local heat transfer rate are defined as

$$C_{fx}=\frac{\tau_w}{\rho_f U^2}, \qquad Nu_x=\frac{\bar{x}q_w}{\kappa_f(T_w-T_\infty)}, \tag{10}$$

for wavy texture q_w and τ_w are described as

$$\tau_w=\mu_{nf}(\nabla\bar{u}.\hat{n})_{y=0}, \qquad q_w=-\kappa_{nf}(\nabla T.\hat{n})_{y=0}, \tag{11}$$

where wavy texture normal vector is $\hat{n}=(-\frac{S_\xi}{\mathcal{H}},\frac{1}{\mathcal{H}})$ and final form for C_{fx} and Nu_x take the form

$$C_f=C_{fx}(Gr/x)^{\frac{1}{4}}=\frac{\mathcal{H}}{(1-\phi)^{2.5}}f''(\xi,0), Nu=Nu_x(Grx^3)^{-1/4}=\mathcal{H}\frac{\kappa_{nf}}{\kappa_f}\theta'(\xi,0). \tag{12}$$

3. Solution methodology and code validation

An elegant, implicit finite difference procedure to solve the coupled PDEs (7) and (8) along with BCs (9). The detailed procedure can be seen in the refs. [32, 33]. This scheme is particularly suitable for parabolic nature boundary layer fluid flow problems and extensively used in computational fluid dynamics. It is unconditionally stable and fast second-order convergence for highly coupled fluid flows. It includes the following main four steps:

1) Reduction of the N^{th} order PDEs system to N first-order ODEs.

2) Use finite difference approximation to transform finite difference equations.

3) Newton method for linearization of non-linear algebraic equations.

4) Block-tridiagonal elimination technique is adopted for solving linearized algebraic equations.

The linearized algebraic equations are solved iteratively. The same process is repeated until the relative difference between the current and the previous iteration up to 10^{-5}. The solution is supposed to have converged and the iterative process is stopped. The flow chart of the Keller-box scheme is demonstrated below:

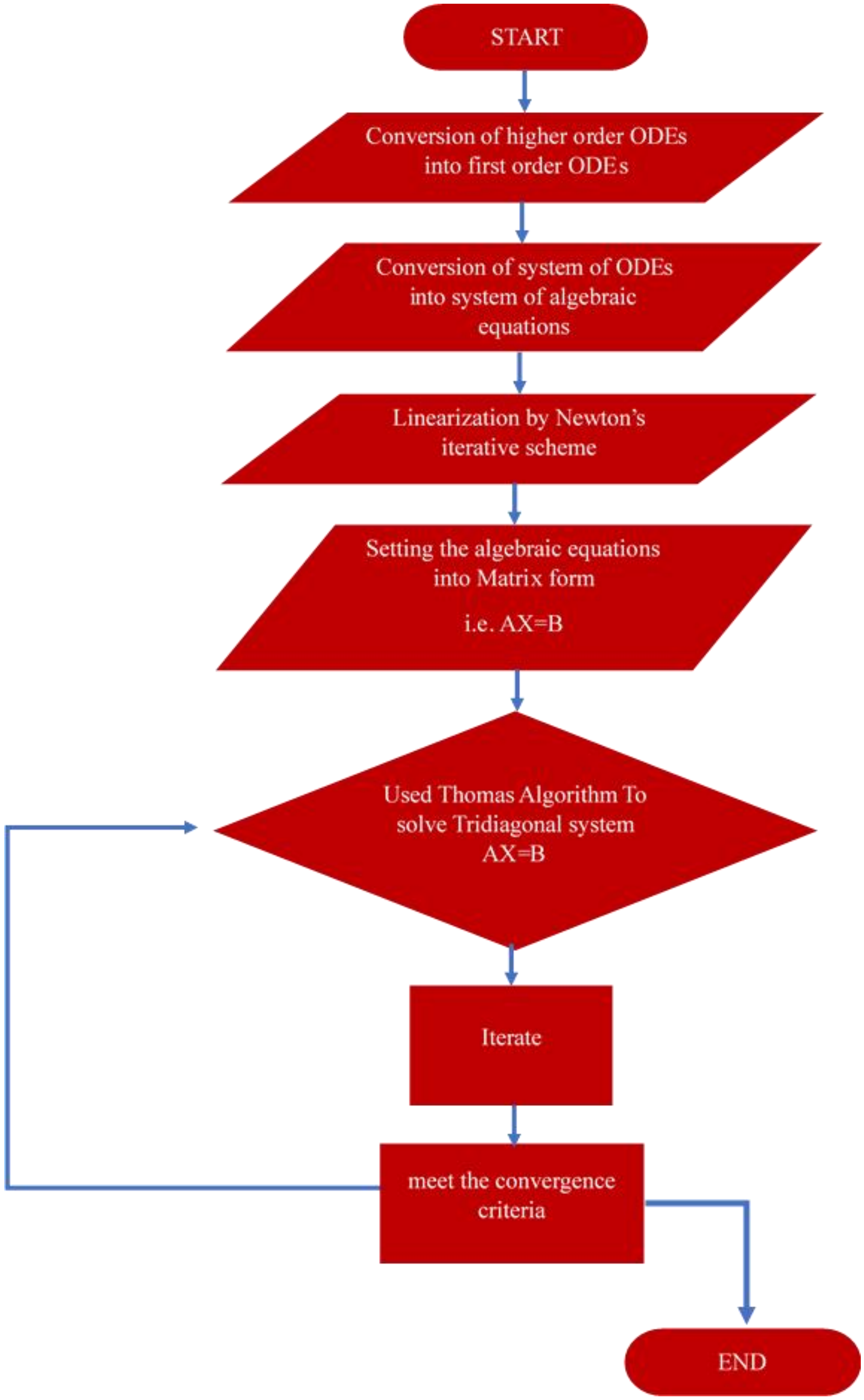

In order to authenticate the accuracy of the current procedure, we have compared our results for the C_f and Nu, for various Prandtl numbers are listed in Tables 1 and 2. The matching in all the overhead cases are shown to be superb with the results established by Alim et al. [34] and Hossain et al. [35].

Table 1: Computed values of $f''(0,0)$ and $-\theta'(0,0)$, for different Pr when $\alpha = \beta = \xi = 0$.

Pr	$f''(0,0)$			$-\theta'(0,0)$		
	present	Hossain et.al. [35]	Alim et al. [34]	Present	Hossainet.al. [35]	Alim et al. [34]
1	0.9082	0.908	0.90814	0.4010	0.401	0.40101
10	0.5928	0.591	0.59269	0.8268	0.825	0.82663
25	0.4876	0.485	0.48733	1.0690	1.066	1.06847
50	0.4176	0.485	0.41727	1.2896	1.066	1.28879
100	0.3559	0.352	0.35559	1.5495	1.542	1.54827

Table 2: Tabulated data for C_f and Nu for different Pr when $\alpha = 0.2, \beta = 0,\ \xi = 2.0$.

Pr	C_f		Nu	
	present	Alim et al. [33]	Present	Alim et al. [33]
0.72	0.74643	0.74641	0.33683	0.33715
1.5	0.66054	0.6690	0.43354	0.43391
3.0	0.58201	0.58220	0.54120	0.54159
4.5	0.53822	0.53827	0.61241	0.61277
7.0	0.49270	0.49260	0.69782	0.69810

4. Result discussion

It is worth mentioning that the current flow problem transformed into viscous fluid and vertical wavy texture by assuming $\phi = 0$ and $\beta = 0$ converted to vertical wavy texture problem.

Figures 2, 4, and 6 illustrate the influence of wavy amplitude, the concentration of nanoparticles, and cone half-angle on C_f . Figure 2 shows that C_f decreases with the increase of wavy amplitude. C_f is minimum for TiO_2, maximum for $Cu - TiO_2$ hybrid nanoparticle. Figure 4 reveals that C_f is the minimum for plain fluid and rises with the inclusion of nanoparticles. C_f is minimum for TiO_2, maximum for $Cu - TiO_2$ hybrid nanoparticle. Figure 6 represents that C_f enhances with the decrease of cone half-angle. Once again C_f is minimum for TiO_2 then for $Cu - TiO_2$ hybrid nanoparticle. The reason behind that the nanoparticles in the base fluid cause some change in the flow characteristics in terms of shear stress as observed from these figures. This is due to the increase in the viscosity of the base fluid. By considering the proportion of the volumetric fraction of the nanoparticles in the hybrid nanofluid the friction factor can be adjusted to increase the heat transfer rate for the practical situations. The heat transfer rate in terms of Nusselt number Nu for various parameters namely, wavy amplitude, the concentration of nanoparticles, and cone half-angle are plotted in figures 3, 5, and 7. It is seen from Figure 3 that Nu reduces with the increase of wavy amplitude. Nu is minimum for TiO_2, maximum for $Cu - TiO_2$ hybrid nanofluid. Figure 5 shows that Nu is minimum for plain fluid and increases for $Cu - TiO_2$ hybrid nanofluid. Figure 7 depicts that Nu enhances with the reduction of the cone half-angle. Nu is minimum for TiO_2 and $Cu - TiO_2$ hybrid nanoparticle at ratio 5%:5% concentration of nanoparticle.

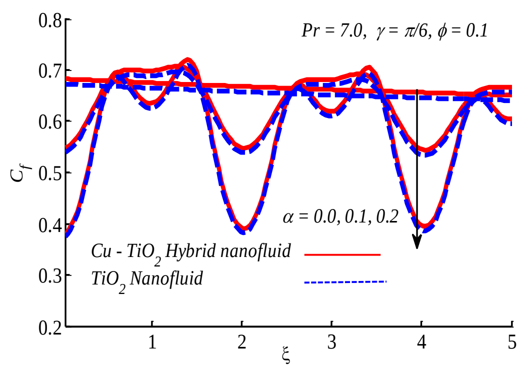

Fig. 2: Effect of waviness on skin friction.

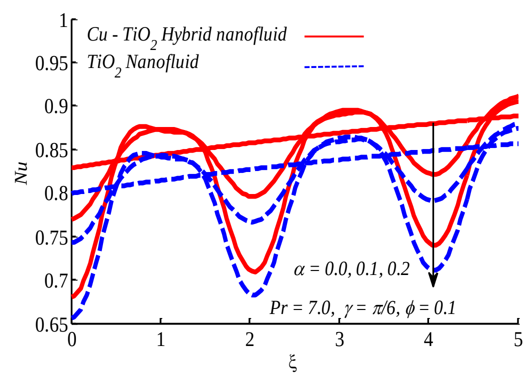

Fig. 3: Effect of waviness on Nusselt Number.

This is because Nusselt number is depending upon different factors such as the concentration of nanoparticles, random movement of particles due to the Brownian diffusion and thermophoresis rises the viscosity and thermal conductivity of nanofluid The Figures reveals that the rate of heat transfer in terms of Nusselt number enhances for hybrid nanofluid in comparison to water and TiO_2/water nanofluid by adding a small number of copper nanoparticles.

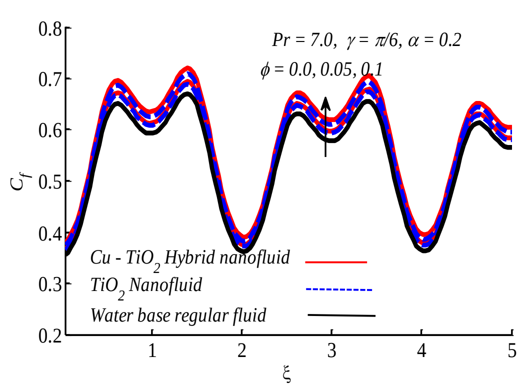

Fig. 4: Graph of skin friction influenced by ϕ.

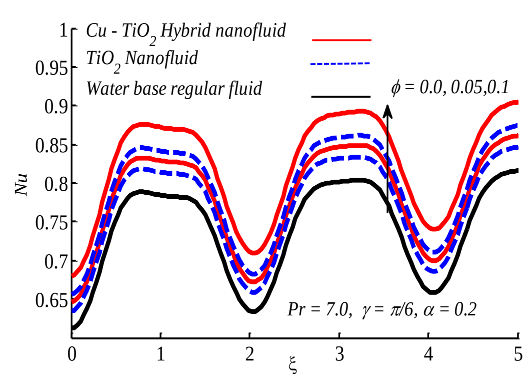

Fig. 5: Graph of Nusselt number influenced by ϕ.

C_f against wavy amplitude and concentration of nanoparticles are shown in Figures 8 and 10. Figure 8 follows that C_f reduces with the increase of wavy amplitude. Figure 10 depicts C_f upturns with incrementing the concentration of nanoparticle. The same reason that inclusion of nanoparticle strengthens the viscosity of the base fluid and hence fluid friction signifies. The graph of Nu versus wavy amplitude, the concentration of nanoparticles is plotted in Figures 9 and 11. It can be seen from Figure 9 that follows that Nu varies linearly with the increase of wavy amplitude. Figure 10 depicts C_f upturns with incrementing the concentration of nanoparticle. The same reason that inclusion of nanoparticle strengthens the viscosity of the base fluid and hence fluid friction increases. C_f is minimum for TiO_2, it increases for $Cu - TiO_2$ hybrid nanofluid. Variation of Nu concerning α and ϕ are shown in Figures 9 and 11. Nu varies linearly with the increase of α whereas exponentially increase is depicted in figure 11 in the case of ϕ. Heat transfer is minimum for TiO_2, almost equal in the case of $Cu - TiO_2$ hybrid nanofluid.

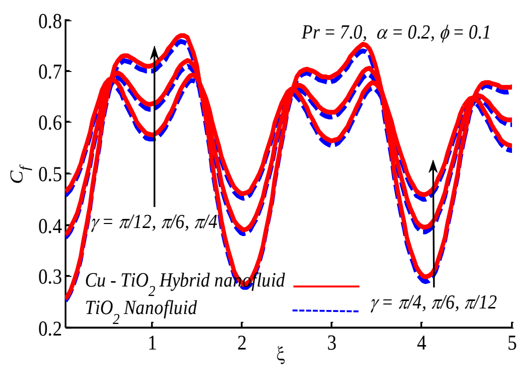

Fig. 6: Graph of skin friction influenced by γ.

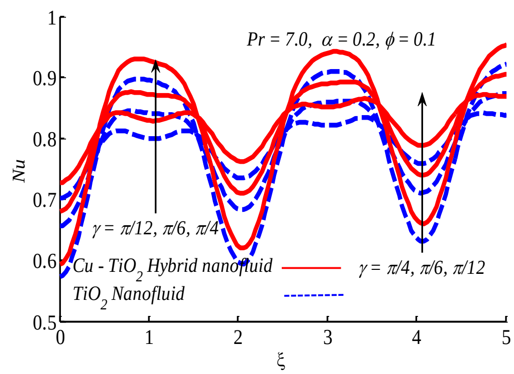

Fig. 7: Graph of Nusselt number influenced by γ.

Table 3: Thermophysical properties of base fluid and nanoparticle.

Properties	*Cp (J/kgK)*	*ρ(kg/m3)*	*k(W/mK)*	β *10^-5(1/K)
Fluid(water)	4179	997.1	0.613	21.00
Cu	383.1	8954	386	1.67
TiO_2	686.2	4250	8.9538	0.9

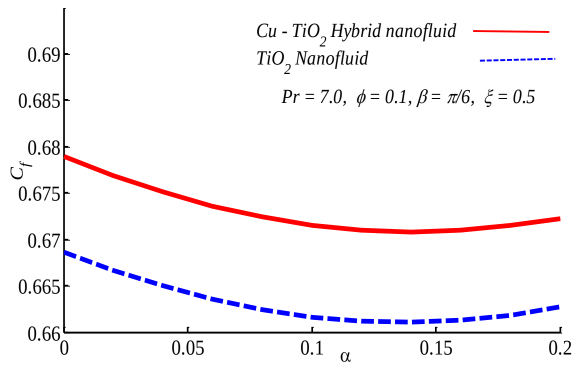

Fig. 8: Skin friction graph verses α.q

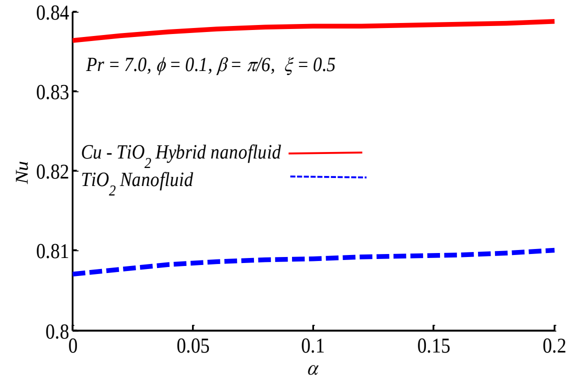

Fig. 9: Nusselt number against α.

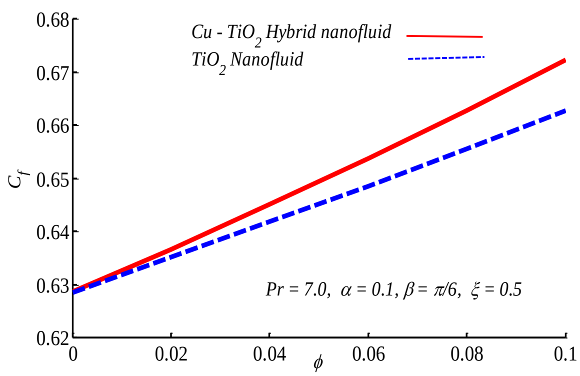

Fig. 10: Skin friction variation against ϕ.

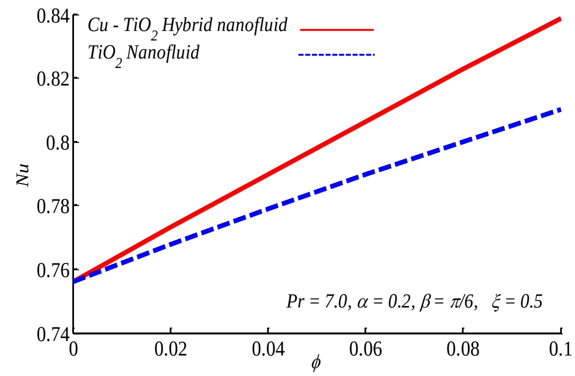

Fig. 11: Nusselt number variation for different ϕ.

Conclusions

In this research article, we have investigated natural convection heat transfer of $Cu - TiO_2$ hybrid nanofluid past wavy truncated cone wavy texture. Using suitable transformations the PDEs are converted to compact non-similar nature system of PDEs. The system is solved by an appropriate and accurate Keller-box technique having second degree of convergence. The results show accurate matching with the previous results which confirm the rationality of the code and presented data. The key outcomes of this analysis are

(i) The local skin friction increases and the Nusselt number decreases by increasing the values of wavy amplitude.

(ii) An increase in the concentration of nanoparticles in the base fluid produces an increase in the skin friction coefficient and the local Nusselt number.

(iii) A rise in the truncated cone half-angle leads to the increase in skin friction and Nusselt number.

(iv) Titania – water nanofluid has lower heat transfer rates as compared to copper-titania hybrid nanofluid.

(v) The increasing of the truncated cone half-angle enhances the heat transfer rates.

(vi) Additionally, this analysis illustrates that the hybrid nanofluid will be very significant in the cooling and heating processes.

References

1. Na, T.Y. and Chiou, J.P., 1979. Laminar natural convection over a frustum of a cone. Applied Scientific Research, 35(5-6), pp.409-421.
2. Na, T.Y. and Chiou, J.P., 1979. Laminar natural convection over a slender vertical frustum of a cone. Wärme-und Stoffübertragung, 12(2), pp.83-87.
3. Singh, P., Radhakrishnan, V. and Narayan, K.A., 1989. Natural convection flow over a vertical frustum of a cone for constant wall heat flux. Applied scientific research, 46(4), pp.335-345.
4. Singh, P., Radhakrishnan, V. and Narayan, K.A., 1989. Non-similar solutions of free convection flow over a vertical frustum of a cone for constant wall temperature. Ingenieur-Archiv, 59(5), pp.382-389.
5. Pop, I. and Na, T.Y., 1999. Natural convection over a vertical wavy frustum of a cone. International journal of non-linear mechanics, 34(5), pp.925-934.
6. Yih, K.A., 1999. Effect of radiation on natural convection about a truncated cone. International Journal of Heat and Mass Transfer, 42(23), pp.4299-4305.
7. Chamkha, A.J., 2001. Coupled heat and mass transfer by natural convection about a truncated cone in the presence of magnetic field and radiation effects. Numerical Heat Transfer: Part A: Applications, 39(5), pp.511-530.
8. Hossain, M.A., Munir, M.S. and Takhar, H.S., 2000. Natural convection flow of a viscous fluid about a truncated cone with temperature dependent viscosity. Acta Mechanica, 140(3-4), pp.171-181.
9. Postelnicu, A., 2006. Free convection about a vertical frustum of a cone in a micropolar fluid. International journal of engineering science, 44(10), pp.672-682.
10. Cheng, C.Y., 2008. Natural convection of a micropolar fluid from a vertical truncated cone with power-law variation in surface temperature. International communications in heat and mass transfer, 35(1), pp.39-46.

11. Cheng, C.Y., 2009. Nonsimilar boundary layer analysis of double-diffusive convection from a vertical truncated cone in a porous medium with variable viscosity. Applied mathematics and computation, 212(1), pp.185-193.
12. Cheng, C.Y., 2011. Natural convection boundary layer flow of a micropolar fluid over a vertical permeable cone with variable wall temperature. International Communications in Heat and Mass Transfer, 38(4), pp.429-433.
13. Srinivasa, A.H. and Eswara, A.T., 2016. Effect of internal heat generation or absorption on MHD free convection from an isothermal truncated cone. Alexandria engineering journal, 55(2), pp.1367-1373.
14. Cheng, C.Y., 2013. Free convective boundary-layer flow over a vertical truncated cone in a bidisperse porous medium. In Proceedings of the World Congress on Engineering (Vol. 3).
15. Pătrulescu, F.O., Groşan, T. and Pop, I., 2014. Mixed convection boundary layer flow from a vertical truncated cone in a nanofluid. International Journal of Numerical Methods for Heat & Fluid Flow.
16. Siddiqa, S.; Begum, N.; Hossain, M.A.; Mustafa, N.: Two-phase dusty fluid flow along a cone with variable properties. Heat Mass Transf. 53, 1517–1525 (2017)
17. Amanulla, C.H., Nagendra, N. and Suryanarayana Reddy, M., 2017. Thermal and momentum slip effects on hydromagnetic convection flow of a Williamson fluid past a vertical truncated cone. Frontiers in Heat and Mass Transfer (FHMT), 9(1).
18. Ahmed, S.E. and Mahdy, A., 2012. Natural convection flow and heat transfer enhancement of a nanofluid past a truncated cone with magnetic field effect. World Journal of Mechanics, 2(05), p.272.
19. Siddiqa, S., Begum, N., Iftikhar, T., Rafiq, M., Hossain, M.A. and Gorla, R.S.R., 2019. Thermal Radiation Effects on Casson Dusty Boundary-Layer Fluid Flow Along an Isothermal Truncated Vertical Cone. Arabian Journal for Science and Engineering, 44(9), pp.7833-7842.
20. Siddiqa, S., Begum, N., Hossain, M.A., Shoaib, M. and Reddy Gorla, R.S., 2018. Radiative heat transfer analysis of non-Newtonian dusty Casson fluid flow along a complex wavy surface. Numerical Heat Transfer, Part A: Applications, 73(4), pp.209-221.
21. Siddiqa, S., Begum, N., Hossain, M.A. and Massarotti, N., 2016. Influence of thermal radiation on contaminated air and water flow past a vertical wavy frustum of a cone. International Communications in Heat and Mass Transfer, 76, pp.63-68.

22. Mahdy, A. and Elshehabey, H.M., 2018. Gyrotactic microorganisms free convection boundary layer flow about a vertical truncated cone in nanofluid porous media. Latin American Applied Research-An international journal, 48(1), pp.57-62.
23. Ram Reddy, C. and Rao, C.V., 2017. Non-similarity Solutions for Natural Convective Flow of a Nanofluid Over Vertical Frustum of a Cone Embedded in a Doubly Stratified Non-Darcy Porous Medium. International Journal of Applied and Computational Mathematics, 3(1), pp.99-113.
24. Siddiqa, S., Begum, N., Hossain, M.A. and Gorla, R.S.R., 2017. Numerical solutions of natural convection flow of a dusty nanofluid about a vertical wavy truncated cone. Journal of Heat Transfer, 139(2).
25. Ghaffari, A., Mustafa, I., & Javed, T. (2019). Influence of nonlinear radiation on natural convection flow of carbon nanotubes suspended in water-based fluid along a vertical wavy surface. Physica Scripta, 94(11), 115214.
26. Iqbal, M. S., Mustafa, I., & Ghaffari, A. (2019). Analysis of Heat Transfer Enrichment in Hydromagnetic Flow of Hybrid Nanofluid Along Vertical Wavy Surface. Journal of Magnetics, 24(2), 271-280.
27. Ghaffari, A., Javed, T., Mustafa, I., & Labropulu, F. (2018). Modeling and simulation of natural convection flow along a rough surface of sinusoidal nature with variable heat flux: Using Keller box scheme. Thermal Science, (00), 106-106.
28. Mustafa, I., Javed, T., & Ghaffari, A. (2017). Hydromagnetic natural convection flow of water-based nanofluid along a vertical wavy surface with heat generation. Journal of Molecular Liquids, 229, 246-254.
29. Javed, T., Ahmad, H., & Ghaffari, A. (2016). Influence of radiation on vertical wavy surface with constant heat flux: Using Keller box scheme. Alexandria Engineering Journal, 55(3), 2221-2228.
30. Siddiqa, S., Begum, N. and Hossain, M.A., 2016. Radiation effects from an isothermal vertical wavy cone with variable fluid properties. Applied Mathematics and Computation, 289, pp.149-158.
31. Tiwari, R. K., and Das, M. K. (2007). Heat transfer augmentation in a two-sided lid-driven differentially heated square cavity utilizing nanofluids. *International Journal of heat and Mass transfer*, *50*(9-10), 2002-2018.
32. Na, T.Y. ed., 1980. Computational methods in engineering boundary value problems. Academic Press.

33. Cebeci, T. and Bradshaw, P., 2012. Physical and computational aspects of convective heat transfer. Springer Science & Business Media.
34. Alim M.A., Karim M.R. and Akand M.M. (2012) Heat generation effects on magnetohydrodynamic (MHD) natural convection flow along a vertical wavy surface with variable thermal conductivity. A. J. of Comput. Math., 2 , 42-50.
35. Hossain, M. A., Kabir, S., & Rees, D. A. S. (2002). Natural convection of fluid with variable viscosity from a heated vertical wavy surface *ZAMP*, *53*(1), 48-57.

Submitted: 22.08.2020

Revised: 07.10.2020.

Accepted: 10.10.2020.